Research Article | Open Access

Journal of Environmental Exposure Assessment

Wang *et al. J. Environ. Expo. Assess.* **2026**, *5*, 30 **DOI:**10.20517/jeea.2026.32

Global associations between extreme temperature events and childhood cancer incidence and mortality

Minghao Wang[1,2,#], Ruiqi Gu[2,#], Qingyang Zhu[3,#], Yingya Zhao[2], Liyi Zhang[1], Wenjuan Ma[4], Zhouguang Hui[5], Tiantian Li[6], Yunhui Zhang[1,2,4]

Keywords:
Extreme temperature, childhood cancer burden, GBD, spatiotemporal analysis

Citation: Wang, M.; Gu, R.; Zhu, Q.; Zhao, Y.; Zhang, L.; Ma, W.; Hui, Z.; Li, T.; Zhang, Y. Global associations between extreme temperature events and childhood cancer incidence and mortality. *J. Environ. Expo. Assess.* **2026**, *5*, 30. https://dx.doi.org/10.20517/jeea.2026.32

Received: 8 Jun 2026
First Decision: 27 Jul 2026
Revised: 5 Sep 2026
Accepted: 7 Sep 2026
Published: 17 Sep 2026

Academic Editor:
Stuart Harrad
Copy Editor:
Pei-Yun Wang
Production Editor:
Pei-Yun Wang

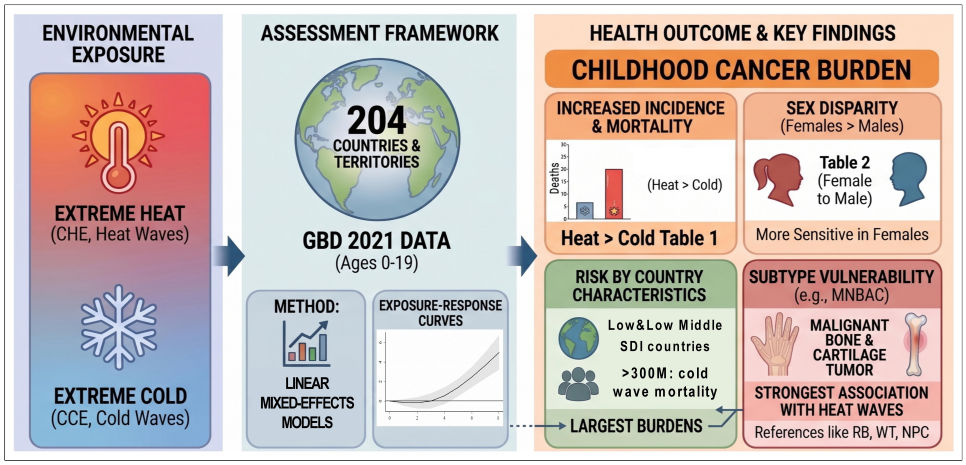

Abstract

Although extreme temperatures are recognized as an environmental threat, their contribution to the global burden of childhood cancer remains poorly quantified. We aimed to estimate childhood cancer incidence and mortality rates associated with heat and cold exposures across 204 countries and territories from 1990 to 2021. Daily ambient temperature series from the U.S. National Oceanic and Atmospheric Administration meteorological stations were used to calculate location-specific cumulative heat exposure, cumulative cold exposure, heat waves and cold waves. National estimates of childhood cancer burden among individuals aged 0-19 years in 204 countries and territories were extracted from the Global Burden of Disease 2021 repository. Linear mixed-effects models were fitted to quantify exposure-outcome associations. Subtype-specific analyses were performed for seven solid tumors. A marked global increase in heat-wave frequency has

[1]Key Laboratory of Health Technology Assessment, National Health Commission of the People's Republic of China, Fudan University, Shanghai 200032, China.
[2]Key Laboratory of Public Health Safety, Ministry of Education, School of Public Health, Fudan University, Shanghai 200032, China.
[3]Gangarosa Department of Environmental Health, Rollins School of Public Health, Emory University, Atlanta, GA 30322, USA.
[4]National Children's Medical Center, Children's Hospital of Fudan University, Shanghai 201102, China.
[5]Cancer Hospital Chinese Academy of Medical Sciences, Beijing 100021, China.
[6]Institute of Environment and Health Related Product Safety, Chinese Center for Disease Control and Prevention, Beijing 100021, China.
[#]These authors contributed equally to this work.

Correspondence to: Prof. Yunhui Zhang, Key Laboratory of Public Health Safety, Ministry of Education, School of Public Health, Fudan University, Shanghai 200032, China. E-mail: yhzhang@shmu.edu.cn; Prof. Tiantian Li, Institute of Environment and Health Related Product Safety, Chinese Center for Disease Control and Prevention, Beijing 100021, China. E-mail: litiantian@nieh.chinacdc.cn; Prof. Zhouguang Hui, Cancer Hospital Chinese Academy of Medical Sciences, Beijing 100021, China. E-mail: drhuizg@163.com

occurred since 1990, particularly in Eastern Europe, Africa, and South Asia. Each additional heat-wave event was significantly associated with 0.32 additional cases per 100,000 population and 19.79 additional deaths per 10,000,000 population. The association with incidence appeared stronger in females than in males. The association of extreme temperatures was predominantly observed in low and low-middle socio-demographic index nations and countries with < 300 million inhabitants, although the heat-wave-associated effect estimate was larger in nations with > 300 million residents. Malignant neoplasms of bone and articular cartilage showed the strongest associations with heat waves. The influence of temperature on the association with childhood cancer burden has strengthened, exhibiting an overall upward trajectory over the study period. This first global analysis demonstrates that extreme temperatures, particularly heat, impose a substantial burden on childhood cancer.

INTRODUCTION

Childhood cancer remains one of the leading causes of mortality among children worldwide, particularly in high-income countries[1]. Despite considerable advances in prevention, diagnosis, and treatment in recent years, the global burden of childhood cancer continues to pose a serious public health challenge[2]. According to recent studies, there were approximately 291,300 new cases globally in 2019, along with 1.8 million prevalent cases and 98,800 deaths. The disability-adjusted life years (DALYs) attributable to these malignancies reached 8.3 million[3]. Furthermore, projections from The Lancet Oncology Commission suggest that an estimated 13.7 million cases will be diagnosed over the next three decades[4], underscoring a substantial and growing threat to global child health and societal development.

As research on childhood cancer continues to advance, an increasing number of potential pathogenic factors are being identified[5-7]. Notably, extreme temperatures have emerged as a key concern in the context of anthropogenic climate change[8]. On the one hand, global climate change has markedly increased the frequency, intensity, and complexity of extreme temperature events globally[9]. Global mean surface temperature increased by 1.1 °C in 2019 relative to the pre-industrial baseline (1880-1900)[10]. The coexistence of extreme high- and low-temperature events is linked to Arctic Amplification, wherein the Arctic warms at a rate 2-3 times greater than the global mean. This amplification weakens the polar vortex, resulting in southward intrusions of frigid air that give rise to more destructive cold waves[11]. On the other hand, children represent a particularly vulnerable subpopulation because of their physiological susceptibility[12]. The immaturity of pediatric thermoregulatory centers compromises thermal adaptation, amplifying their physiological susceptibility to temperature anomalies. Furthermore, children possess a higher body surface area-to-mass ratio and higher basal metabolic rates compared to adults, potentially exacerbating systemic physiological stress during prolonged thermal extremes. During critical developmental windows, these physiological stressors - combined with heightened cell proliferation rates - may render pediatric populations particularly vulnerable to environmentally induced oxidative stress and DNA damage[13]. A critical area of ongoing exploration is the hypothesized oncogenic potential of climate-driven thermal extremes, which provides biological plausibility for the observed epidemiological associations. Emerging evidence indicates that environmental temperature fluctuations can induce aberrant human epigenetic modifications[14]. Consequently, it is biologically plausible to postulate that recurrent heat exposure in a warming climate might increase childhood susceptibility to both solid tumors and hematological malignancies through these epigenetic alterations and potential inflammation-mediated genomic instability.

However, substantial heterogeneity exists in both the sources of temperature data and the operational definitions of thermal extremes across epidemiological studies, complicating cross-regional comparisons of temperature-health associations[15]. Geographic disparities - such as Iceland's absence of locally defined heat waves due to its maritime subarctic climate - challenge the universal applicability of temperature thresholds for health risk assessments. This ambiguity also extends to cold effects. Notably, the Global Burden of

Disease (GBD) 2021 database permits queries on temperature-attributable health outcomes, including childhood cancer; however, risk estimates approximating zero dominate the current evidence base. Furthermore, epidemiological evidence regarding the association between extreme temperatures and various subtypes of childhood cancer remains limited, particularly in the context of developing countries. For example, in the 2021 amendment to the Chinese National Guidelines for the management of pediatric hematological diseases and malignant tumors, 22 subtypes of childhood cancer were explicitly identified based on their high incidence, substantial economic burden, and availability of effective treatments. However, the extent to which these specific subtypes are influenced by extreme temperatures has not yet been established.

The present study aims to investigate the epidemiological associations between extreme temperatures and childhood cancer burden on a global scale, providing population-level evidence that may inform future research into these hypothesized biological mechanisms. Using data from GBD 2021, we quantified the association between multidimensional temperature exposures and childhood cancer burden and extended this association to different subtypes. Our analysis also accounted for cross-climate heterogeneity by optimizing extreme temperature metrics with location-specific percentiles.

EXPERIMENTAL

Estimation of childhood cancer burden

The GBD study constitutes a comprehensive scientific effort to quantify health loss due to diseases, injuries, and risk factors across age groups, sex, and geographic regions. For the first time, GBD 2019 incorporated exposure to high ambient temperatures as a globally assessed risk factor. Data on the disease burden attributable to high temperature for GBD 2021 (https://vizhub.healthdata.org/gbd-results/) were sourced from the publicly accessible GBD Results Tool. This study utilized GBD 2021 data on childhood cancer. Specifically, the study obtained tumor data for individuals aged 0-19 years across all countries for the period 1990-2021, including incidence and mortality rates. This study focuses on seven solid tumor subtypes. Each corresponds to a distinct category in the GBD 2021 classification, and all are consistently defined as specific malignant entities in China's national guidelines for pediatric hematological diseases and malignancies. These subtypes are: neuroblastoma (NBL), malignant neoplasm of bone and articular cartilage (MNBAC), hepatoblastoma (HB), nephroblastoma (WT), retinoblastoma (RB), nasopharyngeal carcinoma (NPC), and thyroid carcinoma (TC). While examining the association of extreme temperatures across all childhood cancer categories, this study conducted detailed analyses specifically for these seven selected solid tumors.

Temperature data

Ambient temperature data were sourced from the globally accessible repository (https://www.ncei.noaa.gov/maps-and-geospatial-products) maintained by the U.S. National Oceanic and Atmospheric Administration (NOAA), which integrates quality-controlled measurements from thousands of weather stations worldwide. Hourly observations from this network were used to extract daily maximum (Tmax) and minimum (Tmin) temperatures for each station. To account for substantial regional climatic heterogeneity, location-specific thresholds for thermal extremes were derived: the 90th percentile of the annual Tmax distribution defined relative heat, while the 10th percentile of the annual Tmin distribution defined relative cold (replacing absolute temperature thresholds). Cumulative heat exposure (CHE) was quantified as the sum of daily degrees exceeding the local 90th percentile threshold. Cumulative cold exposure (CCE) was quantified as the sum of daily degrees below the local 10th-percentile threshold. Extreme temperature events were defined as periods of at least three consecutive days during which the daily Tmax exceeded the 90th percentile (heat wave) or the daily Tmin fell below the 10th percentile (cold wave) of the annual distribution in each country and territory. To generate national-level exposure estimates, a station-to-country aggregation approach was employed. First, the cumulative exposures and the frequencies of extreme temperature events were calculated

independently for each meteorological station based on their location-specific percentile thresholds. Subsequently, these station-level metrics were mapped to their respective countries using spatial overlay analysis. The national exposure estimate for each country was then derived by aggregating the data from all stations within its territorial boundaries, weighted by the total number of stations in that country. This approach ensures that the country-level metrics represent the average exposure captured across all available monitoring sites within the national borders.

Statistical analysis

This study quantified the global burden of childhood cancer through cartographic visualization of age-standardized incidence and mortality rates (1990-2021). Temporal trends were evaluated using estimated annual percentage change (EAPC) methodology, a validated metric for assessing secular variations in epidemiological burden indices[16,17]. We calculated the standard errors and *P*-values for all EAPC estimates using heteroskedasticity- and autocorrelation-consistent (HAC) standard errors, specifically employing the Newey-West estimator. To accurately adjust for the multiple testing conducted independently across 204 countries and territories, we applied the Benjamini-Hochberg procedure to control the false discovery rate (FDR).

This study employed a three-pronged analytical strategy. We first calculated annual estimates of CHE, CCE, and the frequency of heat waves and cold waves. To ensure methodological consistency in the descriptive analyses of exposure and childhood cancer burden, we then quantified extreme temperature exposure metrics using the same methodological approach applied in our assessment of childhood cancer burden. Subsequently, the exposure-response relationships between these environmental stressors and childhood cancer burden were rigorously evaluated. Specifically, linear mixed-effects modeling was chosen for this assessment. This approach was favored for its high interpretability, a critical factor in epidemiological inference. While absolute temperature-health associations are typically non-linear[18,19], this study evaluates threshold-based extreme metrics that isolate exposures strictly beyond thresholds. Evidence indicates that beyond the optimal temperature zone, accumulated thermal stress exhibits a monotonic, approximately linear dose-response relationship with adverse health outcomes on both the hot and cold sides of the temperature-response relationship[20]. The specific main model is as follows:

$$Y_{ct} = \beta_0 + \beta_1 \times ET_{ct} + \beta_2 \times population_{ct} + \beta_3 \times SDI_{ct} + \mu_c + \mu_t + \varepsilon$$

In the model, β_0 denotes the overall intercept, whereas the remaining terms are the fixed-effect coefficients for the corresponding variables. We adjusted for key demographic covariates at the national level, specifically total population size and the socio-demographic index (SDI), given their established potential as direct determinants of population health outcomes. The subscripts c and t index the country and year, respectively. ET_{ct} represents the specific extreme temperature exposure metric for country c in year t. To avoid potential multicollinearity, separate mixed-effects models were fitted independently for each of the four exposure variables. The terms μ_c and μ_t represent the country-specific and year-specific random intercepts, and ε is the residual error term. To explore potential heterogeneity in these associations, stratified subgroup analyses were prespecified and conducted based on sex, SDI level, and population size categories. Countries were stratified into three population size strata: small (< 100 million inhabitants), medium (100-300 million inhabitants), and large (> 300 million inhabitants). In addition, we modeled the exposure-response relationship between extreme temperatures and childhood cancer burden using rigorous curve-fitting techniques. To test the robustness of our findings, a sensitivity analysis was performed by employing a narrower reference temperature range (5th-95th percentiles). Additionally, we performed a sensitivity analysis by excluding countries with populations under 2 million to minimize potential bias from stochastic fluctuations in incidence and mortality rates inherent to small populations.

In the second analytical phase, we conducted longitudinal assessments by fitting separate regression models to annual datasets. This approach was designed to evaluate temporal trends in the association of extreme temperature exposures on GBD burden metrics from 1990 to 2021. To address unmeasured heterogeneity across country-years, we implemented linear mixed-effects models with random intercepts for country. This specification allows baseline disease burden to vary among countries. The models also adjusted for two critical confounders: national population size and SDI. Subsequently, we complemented the parametric modeling with a non-parametric locally weighted scatterplot smoothing (LOWESS) model to graphically characterize potential temporal patterns of disease burden affected by extreme temperatures.

In the final analytical phase, we extended the exposure-response relationships derived from the initial association analysis to evaluate etiologic heterogeneity across the seven pre-specified tumor subtypes. All statistical procedures and visualizations were executed in R (version 4.0.5), using the lmtest, maps, and dlnm packages. The geographic boundaries for the global maps were sourced from the maps package, which provides public domain data fully compliant with all applicable open-source license requirements. Statistical significance was assessed via two-tailed tests with $P < 0.05$ as the prespecified threshold.

RESULTS AND DISCUSSION

Epidemiological trends in the global burden of childhood cancer from 1990 to 2021

In 2021, the highest childhood cancer incidence rates were observed in Europe. Countries with the highest mortality rates are predominantly concentrated among high-resource microstates: San Marino, Andorra, Monaco and Singapore. Interestingly, regions with lower levels of healthcare investment appear to exhibit comparatively lower mortality rates for childhood cancer, presenting an apparent paradox. Poland exhibited the highest incidence rate at 26.0 per 100,000 [95% confidence interval (CI): 21.0-32.0], while Somalia recorded the lowest incidence rate at 0.70 per 100,000 (95%CI: 0.50-0.90). Elevated incidence rates persisted in Kyrgyzstan, Romania, Croatia, and Hungary - countries that also demonstrated high burden in the 1990 baseline assessment. Temporal trend analysis identified significant secular changes during 1990-2021: The fastest increases in incidence occurred in Ecuador (EAPC = 2.05; FDR-adjusted *P*-value = 0.04), India (EAPC = 1.87; FDR-adjusted *P*-value = 9.36×10^{-9}), Cabo Verde (EAPC = 1.63; FDR-adjusted *P*-value = 0.01), Nepal (EAPC = 1.54; FDR-adjusted *P*-value = 0.03), whereas the fastest decreases occurred in Sweden (EAPC = -1.33; FDR-adjusted *P*-value = 1.77×10^{-7}), Georgia (EAPC = -1.04; FDR-adjusted *P*-value = 0.02), Brazil (EAPC = -0.83; FDR-adjusted *P*-value = 4.11×10^{-7}), Japan (EAPC = -0.80; FDR-adjusted *P*-value = 1.26×10^{-3}). Supplementary Figures 1 and 2 detail temporal trends in childhood cancer incidence and mortality. EAPC analysis identified mortality increases during 1990-2021 in Cabo Verde, Egypt, Nepal, Bhutan, and Rwanda. Alarmingly, no country or territory showed a statistically significant reduction in mortality during this period.

In our assessment of the global epidemiology of childhood cancer, we found that since 1990, the global burden of childhood cancer has been continuously increasing. Our findings generally aligned well with a previous investigation using data from GBD 2017. Previous work identified particularly high absolute burdens in China and India[21], whereas our rate-based analysis identified countries such as Poland and Kyrgyzstan as having the highest rates. This is because we have provided an epidemiological description of the rate of childhood cancer in our study, thereby accounting for differences in population size. However, our research has also found marked increases over time in China and India, particularly in childhood cancer incidence in India. In addition, we found that countries with less investment in healthcare, such as Chad, Niger, Liberia, the Democratic Republic of Congo, and Equatorial Guinea, have a lower burden of childhood cancer. This may be related to incomplete cancer registration in these countries. Existing literature documents that childhood cancer registration in low- and middle-income countries faces multifaceted challenges, including insufficient resource allocation, underdeveloped health information infrastructure,

incomplete death records, data inaccuracies, sociocultural barriers, and population displacement or instability due to conflict. This is particularly evident in parts of the Middle East and Africa, where contextual political, social, and economic constraints - coupled with ongoing armed conflicts - have severely compromised or rendered inoperative tumor registry systems in several countries[22-24]. These research results need to be brought to the attention of the health department to strengthen cancer registration and improve burden-estimation models, and emphasize the necessity of developing prevention plans tailored to different national conditions.

Characterization of extreme temperature exposures and extreme temperature events

The study showed that, since 1990, European countries including Lithuania, Luxembourg, Serbia, and Hungary have experienced frequent and intense heat waves, with this pattern most pronounced in Eastern Europe. Global mapping [Figure 1] revealed distinct geographical patterning of heat waves. Longitudinal analysis identified a significant global escalation in heat wave frequency, particularly accelerated across West Africa, South Africa, and South Asia - evidenced by Angola (FDR-adjusted P-value = 0.007), Tanzania (FDR-adjusted P-value = 0.036), Ghana (FDR-adjusted P-value < 0.001), and Myanmar (FDR-adjusted P-value < 0.001) exhibiting the steepest EAPC. Remarkably, very few regions displayed statistically significant declines in heat-wave frequency. By 2021, substantial frequency increases emerged in Central Asia, Canada (FDR-adjusted P-value = 0.02), and China (FDR-adjusted P-value = 0.01) alongside persistently elevated European levels. The distribution of cold waves shifted slightly from their 1990 concentration across Asia, Europe, and North America. In 2021, cold-wave frequency was also high in several countries in Oceania and South America. Globally, cold-wave frequency showed divergent temporal trends, with most regions exhibiting increases despite localized declines (several African nations and Panama). Longitudinal quantification of CCE and CHE showed significantly higher exposure levels in 2021 relative to the 1990 baseline.

Europe experienced relatively high frequencies of recurrent heat and cold waves between 1990 and 2021. This finding aligns with existing literature documenting Europe's climatological distinctiveness amid global warming, wherein continental temperature increases have surpassed those of other landmasses[25,26]. Notwithstanding, absolute temperature maxima and peak heat wave frequency are not uniquely concentrated in Europe. For instance, regions such as the Indo-Gangetic Plain have experienced heat waves of greater intensity than contemporaneous European events[27]. This apparent discrepancy primarily stems from methodological heterogeneity in defining heat waves. We used a percentile-based threshold approach that defines heat waves as periods of ≥ 3 consecutive days with daily maximum temperatures exceeding the 90th percentile of the local reference distribution. Conversely, some studies employ absolute temperature thresholds (e.g., > 40 °C), potentially inflating frequencies in inherently hotter climates. Analogous methodological considerations apply to cold wave definitions[9]. Crucially, our analysis identified accelerated heat wave frequency escalation in Africa and South Asia - a pattern corroborated by recent studies. For example, India has sustained a statistically significant upward trajectory in annual heat wave occurrences since the 1990s[28,29]. Collectively, this evidence underscores a global intensification of thermal extremes in both frequency and severity. Urgent implementation of evidence-based adaptation strategies - including early warning systems, infrastructural interventions, and public health preparedness - is imperative to mitigate the escalating burden of temperature-related morbidity and mortality[12].

Extreme temperature-related childhood cancer burden

Linear mixed-effects analyses demonstrated differential association of extreme temperature exposure on childhood cancer burden [Table 1]. Both CCE and CHE were significantly associated with increased incidence and mortality of childhood tumors. Specifically, per 100,000 population, each 1 °C·day increase in CCE was associated with a rise of 0.020 (95%CI: 0.014-0.026) new cases. Similarly, each 1 °C·day increase in CHE corresponded to an additional 0.013 (95%CI: 0.003-0.023) new cases. Moreover, each additional

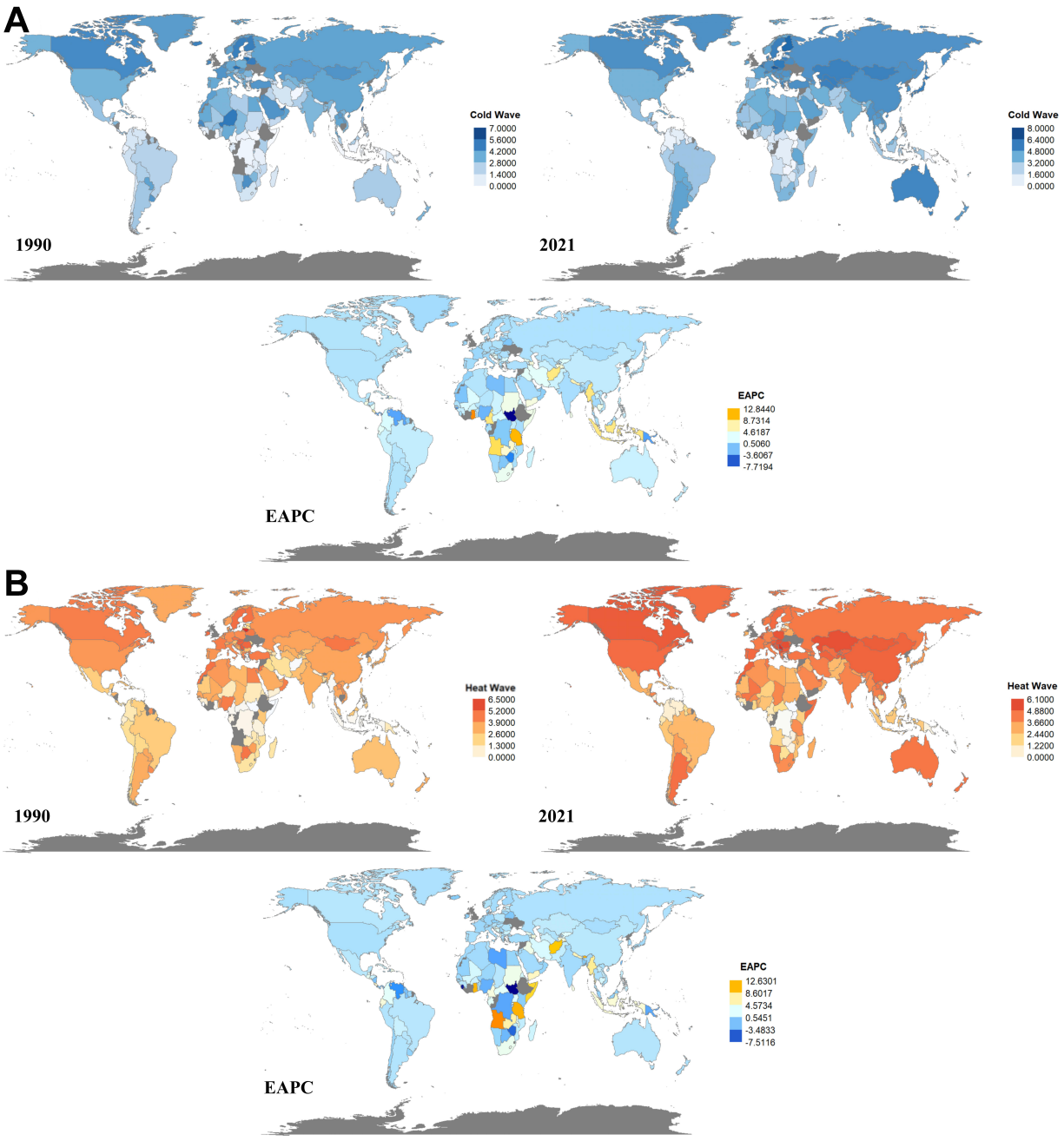

Figure 1. Global spatiotemporal patterns of cold and heat wave frequency, 1990-2021. (A) Global frequency of cold wave: 1990, 2021, and 1990-2021 trend; (B) Global frequency of heat wave: 1990, 2021, and 1990-2021 trend. EAPC: Estimated annual percentage change.

heat-wave event was significantly associated with a rise of 0.32 (95%CI: 0.19-0.45) new cases per 100,000 and 19.79 (95%CI: 1.51-38.08) deaths per 10,000,000. A significant association was also observed between cold-wave frequency and cancer incidence, with an estimated increase of 0.18 (95%CI: 0.05-0.30) new cases per 100,000. Figure 2 delineates exposure-response relationships between extreme temperature metrics and childhood cancer burden, modeled using flexible smoothing splines. These smoothed curves serve as a transparent visual supplement to our primary linear mixed-effects models. As illustrated, while the majority of the exposure-response trajectories exhibit a predominantly linear increase, some localized non-linearities are visually apparent. However, these specific non-linear segments coincide with substantially widened CIs, indicating sparse data and high uncertainty in those extreme ranges. Given that the overarching trend across

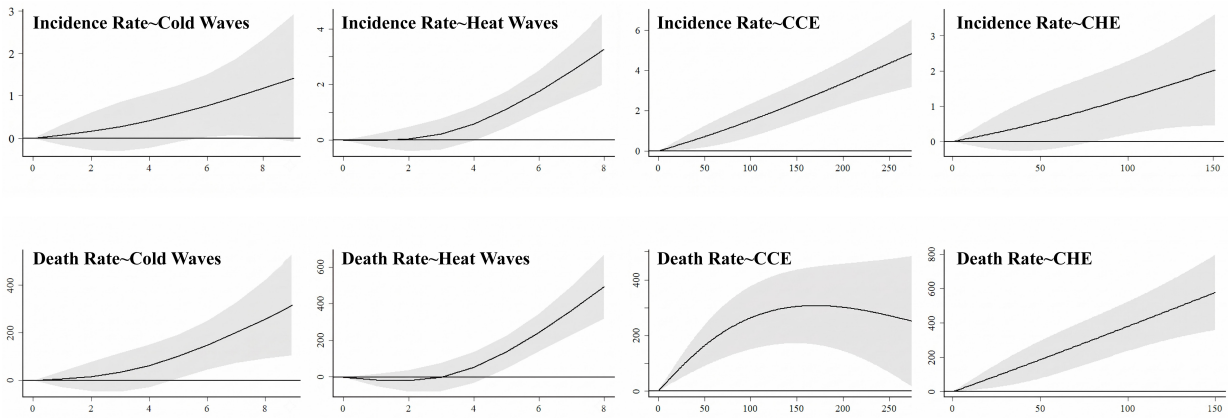

Figure 2. Exposure-response curves for the associations between extreme temperature, extreme temperature events and childhood cancer burden. The shaded area represents the 95%CIs. The x-axis shows the exposure metric (event frequency for heat and cold waves and cumulative exposure for CHE and CCE), measured in °C·day for CCE and CHE, and as the number of occurrences for heat waves and cold spells. The Y-axis represents the absolute change in the childhood cancer incidence and death rate relative to the reference exposure level. Incidence and mortality rates are reported per 100,000 and per 10,000,000 population, respectively. CIs: Confidence intervals; CHE: cumulative heat exposure; CCE: cumulative cold exposure.

Table 1. Association of extreme temperatures and extreme temperature events on childhood cancer burden

	Incidence rate		Mortality rate	
	Estimate	***P*-value**	**Estimate**	***P*-value**
Main model				
CCE	0.020 (0.014, 0.026)	< 0.001	1.029 (0.136, 1.922)	0.02
CHE	0.013 (0.003, 0.023)	0.01	3.408 (1.946, 4.870)	< 0.001
Cold wave	0.176 (0.053, 0.299)	0.01	6.414 (-11.472, 24.301)	0.48
Heat wave	0.320 (0.195, 0.446)	< 0.001	19.793 (1.506, 38.079)	0.03
Sensitivity analysis based on different percentile definitions				
CCE	0.040 (0.027, 0.053)	< 0.001	3.175 (1.285, 5.071)	< 0.001
CHE	0.028 (0.006, 0.051)	0.01	6.442 (3.138, 9.756)	< 0.001
Cold wave	0.343 (0.122, 0.565)	0.002	2.812 (-29.326, 35.049)	0.86
Heat wave	0.533 (0.309, 0.758)	< 0.001	52.971 (20.422, 85.619)	0.001
Sensitivity analysis excluding micro-countries and territories				
CCE	0.034 (0.018, 0.049)	< 0.001	2.196 (1.001, 3.391)	< 0.001
CHE	0.028 (0.018, 0.037)	< 0.001	5.000 (3.099, 6.901)	< 0.001
Cold wave	0.184 (-0.019, 0.384)	0.08	18.060 (-7.061, 43.182)	0.15
Heat wave	0.430 (0.223, 0.634)	< 0.001	38.957 (13.347, 64.567)	0.003

Due to the substantial variance in the magnitude of childhood cancer burden indicators, incidence and mortality rates are reported per 100,000 and per 10,000,000 population, respectively. CCE: Cumulative cold exposure; CHE: cumulative heat exposure.

most metrics remains largely linear, and considering the lack of robust statistical certainty in the non-linear tail regions, the linear models are retained as the primary analytical framework. The sensitivity analyses conducted with varying exposure thresholds produced findings largely congruent with the primary analysis. Moreover, descriptive temporal analysis of annual data suggests that the influence of temperature on the association with childhood cancer burden has generally strengthened, with the association estimates remaining at elevated levels in recent years compared to the 1990 baseline [Figure 3].

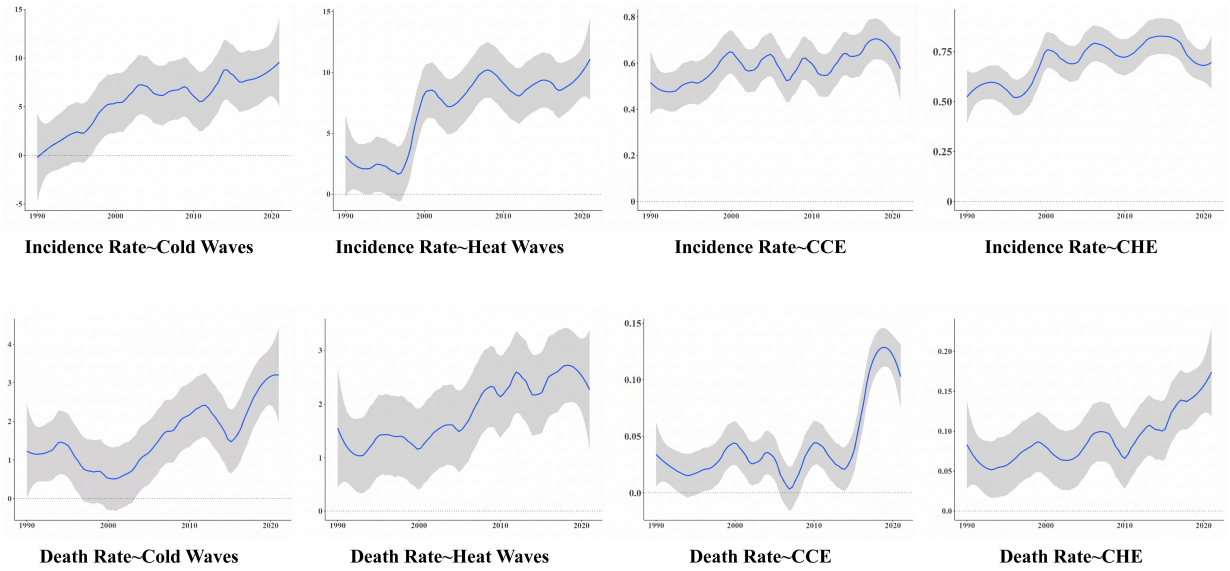

Figure 3. Longitudinal associations between exposure to various extreme temperatures or extreme temperature events and childhood cancer burden. The shaded area represents the 95%CIs. The X-axis indicates the specific year, while the Y-axis illustrates the association of extreme temperature events on the incidence and mortality rates of childhood cancer. Incidence and mortality rates are reported per 100,000 and per 10,000,000 population, respectively. CIs: Confidence intervals; CCE: cumulative cold exposure; CHE: cumulative heat exposure.

Although epidemiological evidence linking extreme temperature to overall childhood cancer risk remains limited, our findings align with subtype-specific studies. For example, a California-based cohort study reported a robust association between high ambient temperature during early gestation and increased risk of childhood acute lymphoblastic leukemia (ALL), suggesting that temperature effects may originate in utero. That study further proposed that sustained prenatal heat exposure potentially disrupts epigenetic regulation in germ cells, thereby promoting ALL pathogenesis[8]. Nevertheless, the precise mechanistic pathways underlying temperature-driven oncogenesis remain elusive. It is crucial to emphasize that the mechanisms discussed below are largely based on biological plausibility derived from adult or *in vitro* models, rather than being experimentally established pathways in pediatric oncology. First, elevated temperatures may promote tumorigenesis via oxidative stress[30], as extreme thermal exposure is known to induce oxidative damage[31-33]. Second, heat exposure has been shown to upregulate various molecular mediators - including epigenetic modifiers, inflammatory markers, heat shock proteins, and stress hormones - which have collectively been associated with an elevated risk of childhood cancer[34-36]. As an exploratory hypothesis to explain why heat exerts a stronger effect than cold, we noted that animal studies indicate cold exposure activates brown adipose tissue (BAT)-mediated glucose uptake, competitively inhibiting tumor proliferation[37]. However, this hypothesis remains highly speculative when extrapolated to human childhood cancers. The generalizability of this phenomenon to pediatric populations is uncertain due to developmental differences in BAT activity and distinct tumor microenvironments in children, and therefore must be interpreted with extreme caution until direct pediatric evidence becomes available.

Stratified association estimates by subgroup

Sex disparities in temperature-related childhood cancer burden revealed distinct patterns [Table 2]: Overall, childhood cancer incidence appeared more strongly associated with extreme temperatures in females than in males. In terms of incidence (per 100,000 population), heat waves significantly increased the incidence of childhood cancer among females (0.45, 95%CI: 0.29-0.60), which was higher than that observed in males (0.20, 95%CI: 0.09-0.31). Similarly, cold wave significantly elevated the incidence in females (0.28, 95%CI: 0.12-0.43), whereas the association was not statistically significant in males (0.08, 95%CI: -0.03-0.19). This

Table 2. Association of extreme temperatures and extreme temperature events on childhood cancer burden and the results of stratification analysis by sex

	Incidence rate			Mortality rate		
	Estimate	***P*-value**	***P* for interaction**	**Estimate**	***P*-value**	***P* for interaction**
CCE						
Male	0.009 (0.004, 0.014)	< 0.001	< 0.001	0.826 (-0.022, 1.675)	0.056	0.48
Female	0.031 (0.023, 0.039)	< 0.001		1.306 (0.290, 2.322)	0.01	
CHE						
Male	0.008 (-0.001, 0.017)	0.07	0.21	3.376 (1.987, 4.764)	< 0.001	0.98
Female	0.018 (0.005, 0.031)	0.01		3.348 (1.683, 5.013)	< 0.001	
Cold wave						
Male	0.082 (-0.025, 0.189)	0.13	0.04	11.559 (-5.436, 28.554)	0.18	0.35
Female	0.276 (0.122, 0.429)	< 0.001		-1.200 (-21.564, 19.165)	0.91	
Heat wave						
Male	0.198 (0.089, 0.308)	< 0.001	0.01	16.335 (-1.042, 33.714)	0.07	0.63
Female	0.447 (0.290, 0.604)	< 0.001		22.942 (2.122, 43.763)	0.03	

Due to the substantial variance in the magnitude of childhood cancer burden indicators, incidence and mortality rates are reported per 100,000 and per 10,000,000 population, respectively. CCE: Cumulative cold exposure; CHE: cumulative heat exposure.

pattern of sex difference was also consistent for CCE. Regarding mortality, although fewer associations reached statistical significance, significant associations with mortality among females were also observed. In contrast, for male children, a significant association with mortality was exclusively observed with CHE, whereas no significant associations were found for the other exposure types. Cold waves did not exhibit any statistically significant association with childhood cancer mortality in either the overall population [Table 1] or the sex-stratified subgroups [Table 2]. Subgroup analyses by population size indicated that CCE and CHE exerted associations across all country groups [Supplementary Table 1]. In contrast, statistically significant associations between heat and cold waves and childhood cancer incidence were more consistently observed across multiple metrics in countries with populations under 100 million and those with 100-300 million people. For instance, in nations with fewer than 100 million people, each increase in cold waves was associated with a rate increase of 5.52 (95%CI: 4.78-6.25) new cases per 100,000, while an increase in heat waves corresponded to a rise of 6.91 (95%CI: 6.15-7.67) new cases. In countries with populations over 300 million, an increase in heat waves led to a substantially larger association estimate of 11.42 (95%CI: 5.94-16.90) new cases per 100,000. Stratification by socioeconomic gradient revealed that childhood cancer burden was more strongly associated with extreme temperatures in low- and low-middle-SDI countries [Supplementary Table 2]. In these countries, heat waves, cold waves, CHE, and CCE were all significantly associated with higher incidence and mortality rates, with heat waves exhibiting the greatest magnitude of association. For example, regarding mortality, heat waves were associated with an increase of 27.29 (95%CI: 18.39-36.20) deaths per 10,000,000 people in low SDI countries, which was substantially lower than the increase of 53.69 (95%CI: 29.90-77.48) deaths observed in low-middle SDI countries.

In subgroup analyses examining the disease burden of childhood cancer associated with extreme temperature exposure, we observed that childhood cancer incidence in females showed greater sensitivity to extreme-temperature exposure than did incidence in males. Physiological differences in thermoregulation and stress responses between sexes may underlie the observed disparity. Females demonstrate divergent thermoregulatory responses to heat, which can result in greater physiological stress during sustained heat waves. Corresponding differences are also likely under cold spells. A proposed mechanism involves X-chromosome gene escape in females, leading to excessive IFN-α production by plasmacytoid dendritic cells

and suggesting a female-specific vulnerability to exaggerated systemic inflammation[38,39]. The systemic inflammation and oxidative stress induced by temperature extremes, when superimposed on the generally heightened immune reactivity in females, could create a more favorable microenvironment for tumor development and progression[40]. Current epidemiological evidence regarding the association between extreme temperature exposure and childhood cancer remains scarce for specific national demographics - particularly countries with populations of 100-300 million and middle SDI countries. Nevertheless, there are still some common patterns across subgroup analyses in different studies. Specifically, countries within the 100-300 million population range often have moderate SDI levels and are undergoing rapid urbanization, yet face critical deficiencies in climate-resilient health infrastructure, including low air-conditioning penetration rates, fragmented pediatric emergency response networks, and limited accessibility to specialized oncology care[41]. Moreover, middle-SDI nations undergoing rapid industrialization may experience a synergistic amplification of pediatric vulnerability due to co-exposure to temperature extremes and industrial pollutants[41,42].

Association of extreme temperatures and specific tumor subtypes

Analysis of different childhood cancer subtypes revealed that NPC, MNBAC, WT, and RB demonstrated greater vulnerability to extreme temperatures [Supplementary Table 3]. Among these, MNBAC showed the strongest associations. For this subtype, each heat wave and cold wave was associated with significant increases in mortality of 2.55 (95%CI: 0.94-4.12) and 1.72 (95%CI: 0.14-3.30) per 10,000,000, respectively. CHE and CCE were also significantly associated with mortality from this subtype. Heat waves and cold waves were also significantly associated with MNBAC incidence; however, these associations should not be interpreted as evidence that temperature events are primary causal factors. For each 1 °C·day increase in cumulative exposure, deaths per 10,000,000 children rose by 0.02 (95%CI: 0.003-0.038) for CHE and 0.01 (95%CI: 0.001-0.021) for CCE with respect to NPC. For WT, the increases were 0.08 (95%CI: 0.03-0.13) and 0.05 (95%CI: 0.01-0.08), respectively.

It is noteworthy that our subtype analysis revealed a counterintuitive negative association between heat and cold waves and HB mortality. This unexpected finding is highly unlikely to reflect a true biological benefit and must be interpreted cautiously. Primarily, HB is a rare pediatric liver malignancy, accounting for approximately 1% to 2% of childhood cancers[43]. In environmental time-series epidemiology, stratifying by exceptionally rare disease outcomes frequently results in minute absolute event counts, which can lead to stochastic statistical fluctuations and unstable, spurious negative point estimates[43]. Furthermore, from a clinical perspective, children diagnosed with HB typically require aggressive multidisciplinary treatments - including intensive chemotherapy, major surgical resections, or liver transplantation - necessitating prolonged stays in highly climate-controlled inpatient facilities or intensive care units[44]. In environmental health research, such prolonged confinement in temperature-regulated institutional microenvironments is a well-documented factor that effectively insulates vulnerable individuals from ambient outdoor temperature extremes, thereby attenuating or distorting the observed epidemiological associations[45]. Consequently, this inverse association likely represents a methodological and clinical artifact rather than a genuine protective effect of extreme weather.

Advantages and limitations

Of note, this represents the first comprehensive epidemiological investigation to quantify the global childhood cancer burden associated with extreme temperatures. Key strengths include leveraging globally representative spatiotemporal data, conducting subtype-specific assessments, and identifying vulnerable populations via subgroup analyses, providing a robust evidence base for policy prioritization.

However, several methodological limitations warrant consideration. First, macro-ecological spatiotemporal constraints restrict causal inference. Aggregating data at the national level obscures local microclimatic

disparities, while our same-year analytical design cannot account for the long latency period of carcinogenesis or specific developmental exposure windows. Thus, our findings represent ecological associations rather than direct causal effects, which are better investigated in future individual-level longitudinal cohorts.

Second, global data availability constraints over the 32-year period necessitated reliance on GBD-modeled estimates, which vary in quality across resource-limited nations. Crucially, because we utilized mean estimates, our reported CIs capture only statistical modeling error and do not propagate the inherent uncertainty bounds of the underlying GBD or exposure data. Furthermore, restricting our confounder adjustment to broad proxies precludes explicit adjustment for dynamic co-exposures like air pollution, leaving room for residual confounding.

Finally, analytical and statistical simplifications may obscure complex dynamics. Relying on a single EAPC metric for temporal trends and assuming linear exposure-response relationships limit more granular interpretation. Additionally, subtype-specific analyses for exceptionally rare malignancies are highly susceptible to sparse data bias and unmeasured confounding from recent treatment advances, which can occasionally yield statistical artifacts. Future studies utilizing Joinpoint regression are warranted to statistically identify structural trend breaks.

Despite these constraints, this study utilizes the most representative global population health data currently available to highlight an emerging environmental threat.

CONCLUSIONS

This multi-national study quantifies the association between extreme temperatures and childhood cancer burden across 204 countries and territories. Our research indicates a rising global burden of childhood tumors between 1990 and 2021, most notably in Europe, a trend that parallels the marked global increase in heat-wave frequency since 1990, particularly in Eastern Europe, Africa, and South Asia. Our findings highlight a divergence in the impact of different thermal extremes. While heat exposure significantly increases both the incidence and mortality of childhood cancer, the evidence supporting an association between cold extremes - particularly cold waves - and mortality remains limited and statistically uncertain. Furthermore, our study identifies key vulnerabilities: the childhood cancer burden associated with abnormal temperatures warrants particular attention in low- and low-middle-SDI countries, and protective measures should specifically consider the greater susceptibility observed in female children.

DECLARATIONS

Acknowledgments

We thank BioRender (https://app.biorender.com/) for providing the platform used to create the Graphical Abstract [Created in BioRender. Zhang, Y. (2026) https://BioRender.com/nbrbu5w].

Authors' contributions

Accessed and verified the underlying data, conducted the formal analysis, and contributed to the original draft: Wang, M.; Gu, R.

Contributed to writing - review and editing: Zhu, Q.

Contributed to supervision and conceptualization: Zhao, Y.; Zhang, L.; Ma, W.

Contributed to methodology, project administration, supervision and writing - review and editing: Hui, Z.; Li, T.; Zhang, Y.

Availability of data and materials

The original contributions presented in this study are included in the article and its Supplementary Materials. Further inquiries can be directed to the corresponding authors. The original data presented in the

study are openly available in GBD 2021 and NOAA at https://vizhub.healthdata.org/gbd-results/; https://www.ncei.noaa.gov/maps-and-geospatial-products.

AI and AI-assisted tools statement

Not applicable.

Financial support and sponsorship

This work was supported by the National Key Research and Development Program of China (2022YFC2705004) and the National Natural Science Foundation of China (22576039 and 82273585).

Conflicts of interest

All authors declared that there are no conflicts of interest.

Ethical approval and consent to participate

Not applicable.

Consent for publication

Not applicable.

Supplementary Materials

Supplementary Materials

REFERENCES

1. Siegel, R. L.; Giaquinto, A. N.; Jemal, A. Cancer statistics, 2024. *CA. Cancer. J. Clin.* **2024**, *74*, 12-49. DOI PubMed
2. Gatta, G.; Botta, L.; Rossi, S.; et al.; EUROCARE Working Group. Childhood cancer survival in Europe 1999-2007: results of EUROCARE-5 - a population-based study. *Lancet. Oncol.* **2014**, *15*, 35-47. DOI PubMed
3. Wu, Y.; Deng, Y.; Wei, B.; et al. Global, regional, and national childhood cancer burden, 1990-2019: an analysis based on the Global Burden of Disease Study 2019. *J. Adv. Res.* **2022**, *40*, 233-47. DOI PubMed PMC
4. Atun, R.; Bhakta, N.; Denburg, A.; et al. Sustainable care for children with cancer: a Lancet Oncology Commission. *Lancet. Oncol.* **2020**, *21*, e185-224. DOI PubMed
5. Spector, L. G.; Pankratz, N.; Marcotte, E. L. Genetic and nongenetic risk factors for childhood cancer. *Pediatr. Clin. North. Am.* **2015**, *62*, 11-25. DOI PubMed PMC
6. Abalo, K. D.; Rage, E.; Leuraud, K.; et al. Early life ionizing radiation exposure and cancer risks: systematic review and meta-analysis. *Pediatr. Radiol.* **2021**, *51*, 45-56. DOI PubMed
7. Persson, M. S. M.; Yin, W.; Döring, N.; et al. Gestational age and cancer risk up to young adulthood in Swedish population born 1974 to 2013: a population-based cohort study. *Int. J. Cancer.* **2022**, *150*, 1269-80. DOI PubMed
8. Rogne, T.; Wang, R.; Wang, P.; et al. High ambient temperature in pregnancy and risk of childhood acute lymphoblastic leukaemia: an observational study. *Lancet. Planet. Health.* **2024**, *8*, e506-14. DOI PubMed PMC
9. Perkins-Kirkpatrick, S. E.; Lewis, S. C. Increasing trends in regional heatwaves. *Nat. Commun.* **2020**, *11*, 3357. DOI PubMed PMC
10. Blunden, J.; Boyer, T. State of the Climate in 2021. *Bull. Am. Meteorol. Soc.* **2022**, *103*, S1-465. DOI
11. Cohen, J.; Agel, L.; Barlow, M.; Garfinkel, C. I.; White, I. Linking Arctic variability and change with extreme winter weather in the United States. *Science* **2021**, *373*, 1116-21. DOI PubMed
12. Romanello, M.; di Napoli, C.; Green, C.; et al. The 2023 report of the Lancet Countdown on health and climate change: the imperative for a health-centred response in a world facing irreversible harms. *Lancet* **2023**, *402*, 2346-94. DOI PubMed PMC
13. Tsuzuki-Hayakawa, K.; Tochihara, Y.; Ohnaka, T. Thermoregulation during heat exposure of young children compared to their mothers. *Eur. J. Appl. Physiol. Occup. Physiol.* **1995**, *72*, 12-7. DOI PubMed
14. Xu, R.; Li, S.; Guo, S.; et al. Environmental temperature and human epigenetic modifications: a systematic review. *Environ. Pollut.* **2020**, *259*, 113840. DOI PubMed
15. Vicedo-Cabrera, A. M.; Sera, F.; Guo, Y.; et al. A multi-country analysis on potential adaptive mechanisms to cold and heat in a changing climate. *Environ. Int.* **2018**, *111*, 239-46. DOI PubMed
16. Liu, Q.; Wang, H.; Chen, Z.; et al. Global, regional, and national epidemiology of nasopharyngeal carcinoma in middle-aged and elderly patients from 1990 to 2021. *Ageing. Res. Rev.* **2025**, *104*, 102613. DOI PubMed

17. Nong, J.; Su, C.; Li, C.; et al. Global, regional, and national epidemiology of childhood neuroblastoma (1990-2021): a statistical analysis of incidence, mortality, and DALYs. *EClinicalMedicine* **2025**, *79*, 102964. DOI PubMed PMC
18. Bo, Y.; Zhu, Y.; Lu, R.; et al. Burden of stroke attributable to high ambient temperature from 1990 to 2019: a global analysis. *Int. J. Stroke.* **2023**, *18*, 1121-31. DOI PubMed
19. Zhao, Q.; Guo, Y.; Ye, T.; et al. Global, regional, and national burden of mortality associated with non-optimal ambient temperatures from 2000 to 2019: a three-stage modelling study. *Lancet. Planet. Health.* **2021**, *5*, e415-25. DOI PubMed
20. Gasparrini, A.; Guo, Y.; Hashizume, M.; et al. Mortality risk attributable to high and low ambient temperature: a multicountry observational study. *Lancet* **2015**, *386*, 369-75. DOI PubMed PMC
21. GBD 2017 Childhood Cancer Collaborators. The global burden of childhood and adolescent cancer in 2017: an analysis of the Global Burden of Disease Study 2017. *Lancet. Oncol.* **2019**, *20*, 1211-25. DOI PubMed PMC
22. Abdul-Sater, Z.; Mukherji, D.; Adib, S. M.; et al. Cancer registration in the Middle East, North Africa, and Turkey (MENAT) region: a tale of conflict, challenges, and opportunities. *Front. Oncol.* **2022**, *12*, 1050168. DOI PubMed PMC
23. Abdul-Sater, Z.; Shamseddine, A.; Taher, A.; et al.; ICRIM. Cancer registration in the Middle East, North Africa, and Turkey: scope and challenges. *JCO. Glob. Oncol.* **2021**, *7*, 1101-9. DOI PubMed PMC
24. Ward, Z. J.; Yeh, J. M.; Bhakta, N.; Frazier, A. L.; Atun, R. Estimating the total incidence of global childhood cancer: a simulation-based analysis. *Lancet. Oncol.* **2019**, *20*, 483-93. DOI PubMed
25. Rousi, E.; Kornhuber, K.; Beobide-Arsuaga, G.; Luo, F.; Coumou, D. Accelerated western European heatwave trends linked to more-persistent double jets over Eurasia. *Nat. Commun.* **2022**, *13*, 3851. DOI PubMed PMC
26. García-León, D.; Casanueva, A.; Standardi, G.; Burgstall, A.; Flouris, A. D.; Nybo, L. Current and projected regional economic impacts of heatwaves in Europe. *Nat. Commun.* **2021**, *12*, 5807. DOI PubMed PMC
27. Kumar, P.; Rai, A.; Upadhyaya, A.; Chakraborty, A. Analysis of heat stress and heat wave in the four metropolitan cities of India in recent period. *Sci. Total. Environ.* **2022**, *818*, 151788. DOI PubMed
28. Sharma, S.; Mujumdar, P. Increasing frequency and spatial extent of concurrent meteorological droughts and heatwaves in India. *Sci. Rep.* **2017**, *7*, 15582. DOI PubMed PMC
29. Watts, N.; Amann, M.; Arnell, N.; et al. The 2019 report of The Lancet Countdown on health and climate change: ensuring that the health of a child born today is not defined by a changing climate. *Lancet* **2019**, *394*, 1836-78. DOI PubMed PMC
30. Greaves, M. A causal mechanism for childhood acute lymphoblastic leukaemia. *Nat. Rev. Cancer.* **2018**, *18*, 471-84. DOI PubMed PMC
31. Ebi, K. L.; Capon, A.; Berry, P.; et al. Hot weather and heat extremes: health risks. *Lancet* **2021**, *398*, 698-708. DOI PubMed
32. Ha, S. The changing climate and pregnancy health. *Curr. Environ. Health. Rep.* **2022**, *9*, 263-75. DOI PubMed PMC
33. Prada, D.; Baccarelli, A. A.; Kupsco, A.; Parks, R. M. Climate change and health: understanding mechanisms will inform mitigation and prevention strategies. *Nat. Med.* **2024**, *30*, 1522-4. DOI PubMed PMC
34. He, J. R.; Yu, Y.; Fang, F.; et al. Evaluation of maternal infection during pregnancy and childhood leukemia among offspring in Denmark. *JAMA. Netw. Open.* **2023**, *6*, e230133. DOI PubMed PMC
35. Whitehead, T. P.; Wiemels, J. L.; Zhou, M.; et al. Cytokine levels at birth in children who developed acute lymphoblastic leukemia. *Cancer. Epidemiol. Biomarkers. Prev.* **2021**, *30*, 1526-35. DOI PubMed PMC
36. Timms, J. A.; Relton, C. L.; Sharp, G. C.; Rankin, J.; Strathdee, G.; McKay, J. A. Exploring a potential mechanistic role of DNA methylation in the relationship between in utero and post-natal environmental exposures and risk of childhood acute lymphoblastic leukaemia. *Int. J. Cancer.* **2019**, *145*, 2933-43. DOI PubMed PMC
37. Seki, T.; Yang, Y.; Sun, X.; et al. Brown-fat-mediated tumour suppression by cold-altered global metabolism. *Nature* **2022**, *608*, 421-8. DOI PubMed PMC
38. Souyris, M.; Mejía, J. E.; Chaumeil, J.; Guéry, J. C. Female predisposition to TLR7-driven autoimmunity: gene dosage and the escape from X chromosome inactivation. *Semin. Immunopathol.* **2019**, *41*, 153-64. DOI PubMed
39. Laffont, S.; Rouquié, N.; Azar, P.; et al. X-Chromosome complement and estrogen receptor signaling independently contribute to the enhanced TLR7-mediated IFN-α production of plasmacytoid dendritic cells from women. *J. Immunol.* **2014**, *193*, 5444-52. DOI PubMed
40. Klein, S. L.; Flanagan, K. L. Sex differences in immune responses. *Nat. Rev. Immunol.* **2016**, *16*, 626-38. DOI PubMed
41. GBD 2021 Risk Factors Collaborators. Global burden and strength of evidence for 88 risk factors in 204 countries and 811 subnational locations, 1990-2021: a systematic analysis for the Global Burden of Disease Study 2021. *Lancet* **2024**, *403*, 2162-203. DOI PubMed PMC
42. Perera, F. Pollution from fossil-fuel combustion is the leading environmental threat to global pediatric health and equity: solutions exist. *Int. J. Environ. Res. Public. Health.* **2017**, *15*, 16. DOI PubMed PMC
43. Spector, L. G.; Birch, J. The epidemiology of hepatoblastoma. *Pediatr. Blood. Cancer.* **2012**, *59*, 776-9. DOI PubMed

44. Czauderna, P.; Haeberle, B.; Hiyama, E.; et al. The Children's Hepatic tumors International Collaboration (CHIC): novel global rare tumor database yields new prognostic factors in hepatoblastoma and becomes a research model. *Eur. J. Cancer.* **2016**, *52*, 92-101. DOI PubMed PMC

45. Bouchama, A.; Dehbi, M.; Mohamed, G.; Matthies, F.; Shoukri, M.; Menne, B. Prognostic factors in heat wave related deaths: a meta-analysis. *Arch. Intern. Med.* **2007**, *167*, 2170-6. DOI PubMed